EPJ Web of Conferences **61**, 04019 (2013)
DOI: 10.1051/epjconf/ 20136104019

Prominent outburst of the blazar CTA 102 in 2012.

V.M. Larionov[1], D.A. Blinov[1,6], S.G. Jorstad[1,2], A.P. Marscher[2], M. Villata[3,a], C.M. Raiteri[3], I. Agudo[4,2,7], P.S. Smith[5], D.A. Morozova[1], I.S. Troitsky[1], and D.P. Clemens[2]

[1] *Astron. Inst., St.-Petersburg State Univ., Russia e-mail: vlar@astro.spbu.ru*
[2] *Institute for Astrophysical Research, Boston University, MA, USA*
[3] *INAF, Osservatorio Astrofisico di Torino, Italy*
[4] *Instituto de Astrofisíca de Andalucía, CSIC, Granada, Spain*
[5] *Steward Observatory, University of Arizona, Tucson, AZ, USA*
[6] *University of Crete, Heraklion, Greece*
[7] *Current Address: Joint Institute for VLBI in Europe, Dwingeloo, the Netherlands*

Abstract. After a few years of quiescence, the blazar CTA 102 underwent a large outburst in the fall of 2012. The flare has been tracked from γ-rays to near-infrared, including *Fermi* and *Swift* data as well as polarimetric data from several observatories. An intensive GASP-WEBT collaboration campaign in optical and NIR bands, with the addition of previously unpublished archival data, allows comparison of this outburst with the previous activity period of this blazar in the early 2000s. We find remarkable similarity between the optical and γ-ray behavior of CTA 102 during the outburst, without any time lag between the two light curves, indicating co-spatiality of the optical and γ-ray emission regions. A strong harder-when-brighter spectral dependence is seen both in γ-rays and optical. The polarimetric behavior of CTA 102 during the outburst conforms with a shock-in-jet interpretation.

1 Introduction

The blazar CTA 102 (4C +11.69, 2FGL J2232.4+1143, $z = 1.037$) is a prominent, well-studied quasar. Like other blazars, it is believed that its jet is oriented close to our line of sight, which causes high relativistic beaming of the jet's emission and violent variability at all wavelengths. CTA 102 was first identified as a quasar in [1] and belongs to the OVV (optically violently variable) [2] as well as to the HPQ (high polarized quasars) subclasses [3].

On long-term scales the blazar exhibits rather moderate variability in optical bands. Modest fluctuations about an average magnitude of $B = 17\overset{\mathrm{m}}{.}7$ over a 14 yr range (about 65 observations between 1973 and 1987) were reported by [4]. An overall amplitude $\Delta R = 0\overset{\mathrm{m}}{.}88$ was observed by [5] in 1994-1997. However, occasional sharp flares have also been observed in CTA 102. Variations as high as $\Delta B = 1\overset{\mathrm{m}}{.}07$ in 2 days [4] and $\Delta V = 1\overset{\mathrm{m}}{.}13$ in 3 days [6] were observed in 1978 and 1996, correspondingly. The previously reported historical maximum for the object, $R \approx 14\overset{\mathrm{m}}{.}5$, was reached on Oct. 4, 2004 during a short-term event accompanied by prominent intranight variability [7]. Between that episode and 2012, only modest variability has been seen in the light curve of this blazar (see Fig. 1).

CTA 102 was discovered to be a γ-ray emitter during the early CGRO (EGRET) mission at a level of $(2.4 \pm 0.5) \times 10^{-7}$ph cm^{-2}s^{-1} ($E > 100$ MeV) [8]. It was also detected in the 10 - 30 MeV energy range by CGRO (COMPTEL) [9]. Since the blazar usually persists in a quiescent state, the average γ-ray flux is rather low $(2.9\pm0.2)\times10^{-9}$ph cm^{-2}s^{-1} ($1 < E < 100$ GeV) according to 2FGL catalog [10]. Therefore, accurate relative timing of flux variations in γ-ray and optical bands is only possible during large outbursts. This kind of cross-correlation analysis performed for several other blazars has recently shown that γ-ray and optical flares are usually coincident and associated with the passage of a new knot through the 43-GHz radio core [11, 12]. Similar events may serve as a crucial test for models localizing the γ-ray emission in blazars (e.g., [13]).

In this paper we analyze the largest outburst of CTA 102 to date in the optical and γ-ray bands [14].

2 Observations and data reduction

2.1 Optical and Near-infrared Photometry

The optical and near-IR light curves of CTA 102 during the 2004–2012 time interval are shown in Fig. 1. The GASP-WEBT observations in 2008–2012 were performed in R band at the following observatories: Belogradchik, Calar Alto, Campo Imperatore, Crimean, Lowell (Perkins), Lulin, Mount Maidanak, New Mexico Skies, Roque (Liverpool Telescope), Rozhen, Sabadell, Skinakas, St. Petersburg, Teide (IAC80 and TCS), and Ti-

[a] On behalf of WEBT-GASP collaboration

jarafe. The V and R-band light curves are complemented by data taken at Steward Observatory under a monitoring program in support of the *Fermi* mission. *BVI* photometric data are from St. Petersburg and Lowell observatories. We also use *B* and *R* Mt. Maidanak data during the 2004 outburst.

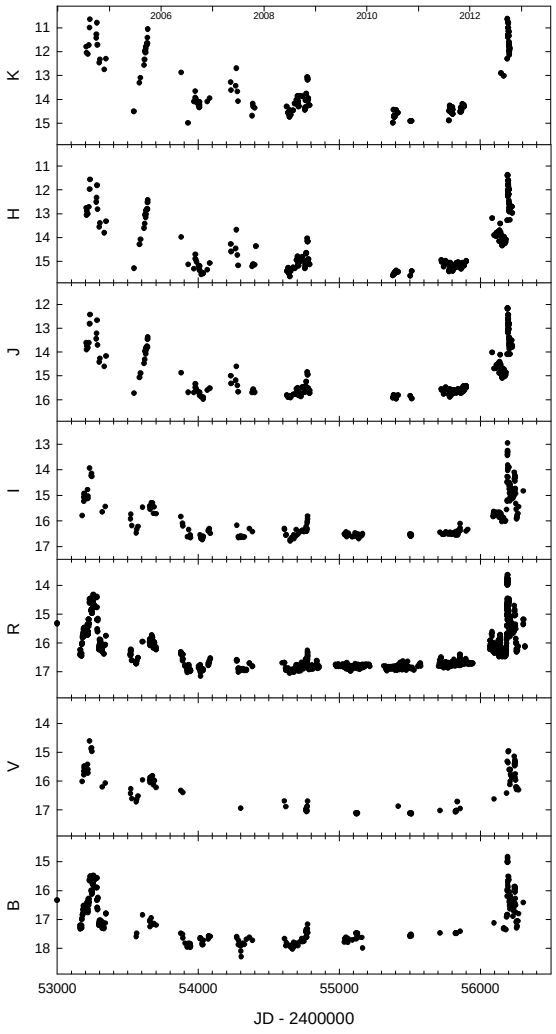

Figure 1. Optical and near-infrared light curves of CTA 102 over the time interval 2004–2013.

2.2 Optical Polarimetry

We use polarimetric data collected at St. Petersburg University (Crimea and St. Petersburg), Lowell (Perkins), Steward and Calar Alto observatories. Instrumental polarization was found via stars located near the object under the assumption that their radiation is unpolarized. The Galactic latitude of CTA102 is -38°and $A_V = 0\overset{m}{.}16$, so that interstellar polarization (ISP) in this direction is less than 0.6%. To correct for ISP, the mean relative Stokes parameters of nearby stars were subtracted from the relative Stokes parameters of the object. This accounts for the instrumental polarization as well. Figure 2 presents the flux and polarization behavior of CTA 102 for 2005–2012. We supplement this plot with a panel showing the γ-ray light curve from *Fermi* LAT in order to show that the most prominent γ-ray activity ever recorded for this source was observed during the September–October 2012 optical outburst. In Fig. 3 we show a blowup of the most active interval of the 2012 outburst. From visual inspection of these figures, it is apparent that during all the time range covered by *Fermi* observations up to the 2012 season, CTA 102 remained inactive both in γ-rays and in optical; the degree of polarization was mostly $\leq$ 10%, while the position angle showed marked ordered variations in the range [-200°, 400°]. We solved the ±180° ambiguity by adding/subtracting 180° each time that the subsequent value of EVPA is > 90° less/more than the preceding one. The onset of the activity in the 2012 season was accompanied by a violent increase of optical polarization activity. The degree of polarization exceeded 20% at some epochs, while the position angle varied over the range of 150° – 300°.

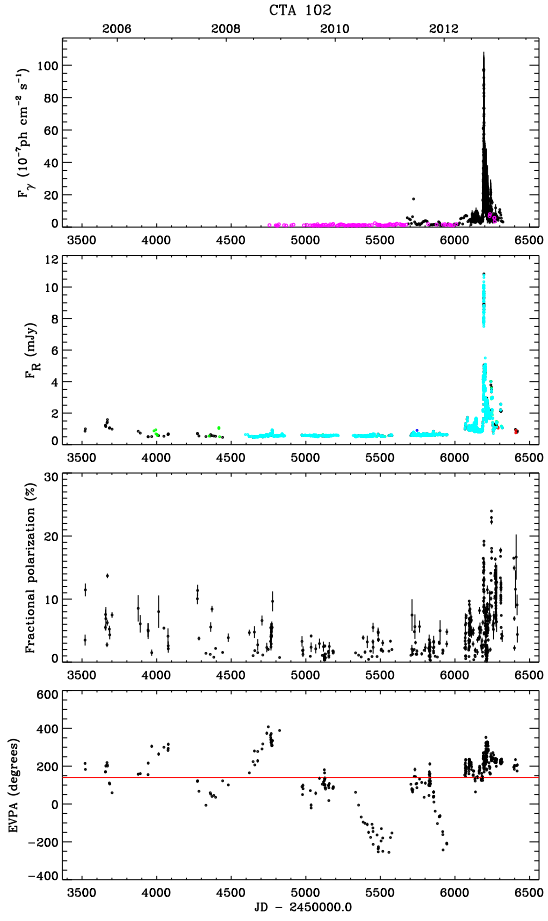

Figure 2. From top to bottom: γ-ray and optical flux evolution, optical fractional polarization and position angle of CTA 102 over the time interval 2004–2013.

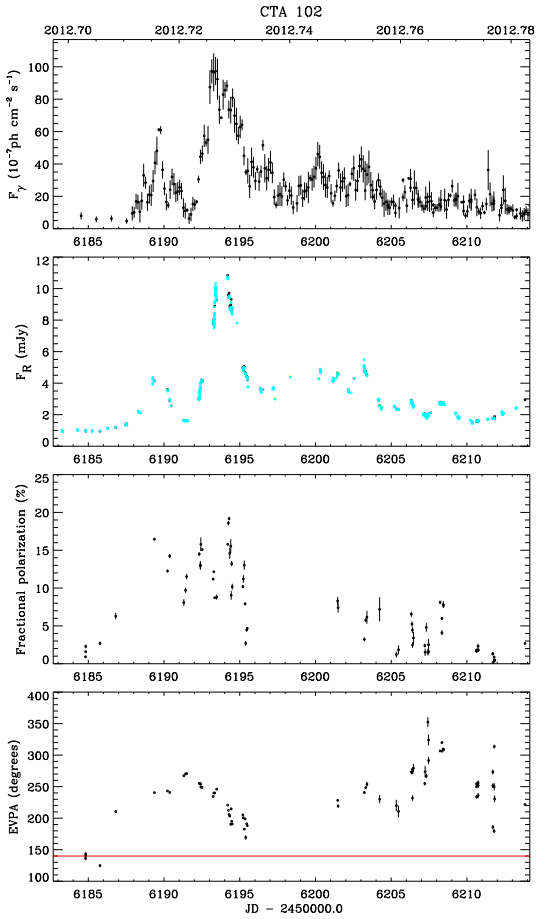

Figure 3. Blowup of Fig. 2 for the 2012 September-October flare.

2.3 Gamma-ray Observations

We analyze *Fermi* LAT data for a field centered on CTA 102 with variable binning, from 1 week to 1 day, depending on the brightness of the object. We also shift the time bins by 6 hr during the huge γ-ray outburst of 2012 September–October, when the flux from the source was higher than 2×10^{-6} ph $\cdot$ cm^{-2}s^{-1}. This prevents missing any possible short-lived events, makes the correlation analysis more robust, and avoids the dependence of the results on the start of the time bins. Despite the high γ-ray flux, we had to increase binning during *Fermi* LAT ToO pointed observations toward S3 0218+35 performed between 2012 September 24 and 30 (JD 2456195–201). We use the standard *Fermi* analysis software package Science Tools `v9r27p1`, with instrument response function `P7SOURCE_V6`, Galactic diffuse emission model `gal_2yearp7v6_v0`, and isotropic background model `iso_p7v6source`. The background models include all sources from the 2FGL catalog within 15° of the quasar. The spectrum of CTA 102 is modelled as a power-law with photon index allowed to vary.

We have calculated the discrete correlation function (DCF) [15] between the optical and γ-ray flux variations of

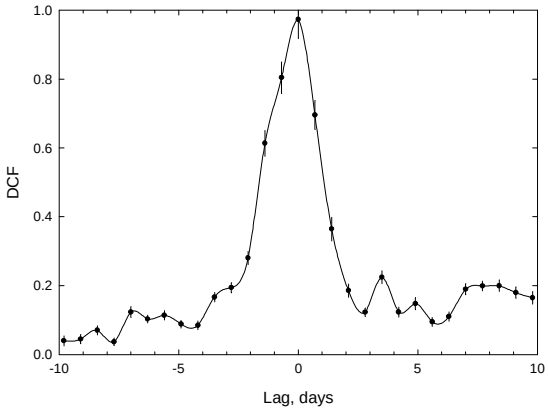

Figure 4. DCF between optical and γ-ray light curves of CTA 102. The lack of delay convincingly demonstrates co-spatiality of active regions.

CTA 102 during 2012. The results, given in Fig. 4, clearly demonstrate that there is no time delay between the variations in the two energy bands to within the accuracy of the DCF method.

2.4 *Swift* Observations

The UVOT observations were performed in the optical *v*, *b*, and *u* bands, as well as in the UV filters *uvw*1, *uvm*2, and *uvw*2. We reduced the data with HEAsoft package version 6.10, with the 20101130 release of the *Swift*/UVOTA CALDB. Multiple exposures in the same filter at the same epoch were summed with `uvotimsum`, and then aperture photometry was performed with the task `uvotsource`. We used Swift calibrations according to [16].

3 Discussion and Conclusions

3.1 Color Evolution

The question of whether a blazar's radiation becomes redder or bluer when it brightens is a topic of numerous papers. It is commonly agreed that the relative contributions of the big blue bump (BBB) and Doppler-boosted synchrotron radiation from the jet and shock wave(s) are different between quiescence and outbursts, and that this leads to variabiity of the SED. The situation is even more complicated, in cases like CTA 102, where broad emission lines contaminate the wide photometric bands (the Mg II λ2800 line is redshifted to λ5600). A straightforward way to segregate the contribution of the component of radiation that is variable on the shortest time scales (presumably, synchrotron radiation) has been suggested in numerous papers by Hagen-Thorn and co-workers; see also [17, 18]. The method is based on plots of (quasi)simultaneous flux densities in different color bands and the construction of the relative SED based on the slopes of the sets of flux-flux relations obtained that way.

An example of such an approach is given in Fig. 5, where the flux densities in *H* and *K* bands are plotted

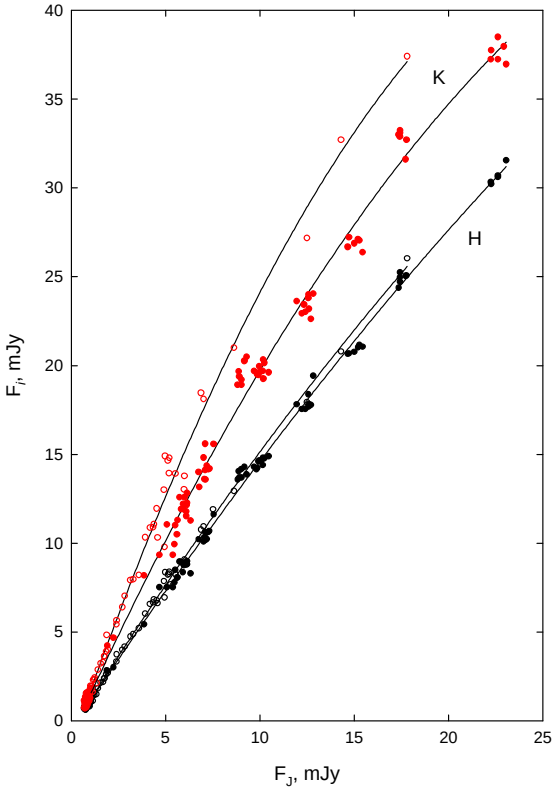

Figure 5. Two-flux near-infrared dependencies. Filled symbols refer to the time interval 2008–2012, open symbols to the 2004 outburst.

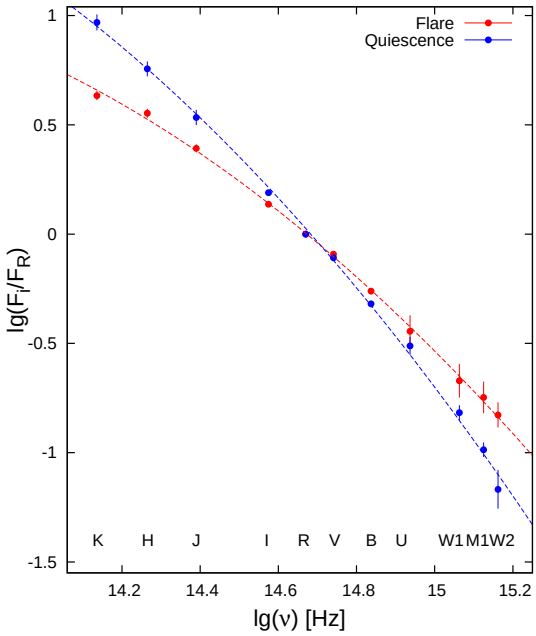

Figure 6. Relative SEDs of the *variable* component in CTA 102 during quiescence (blue) and 2012 flare (red) from NIR to UV.

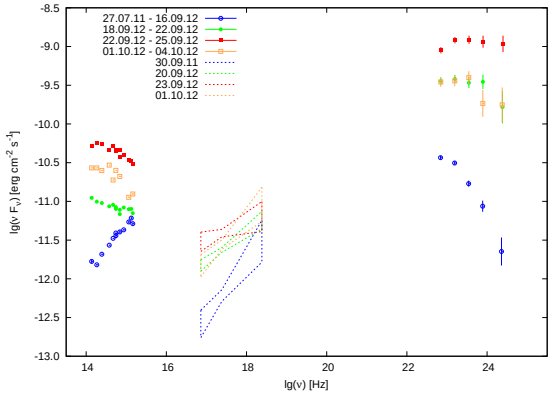

Figure 7. (Quasi)simultaneous SEDs of CTA 102 from NIR to γ-rays.

against J band flux density. This figure demonstrates that the low- and high-flux behaviors either reflect variability of different sources of radiation (e.g., the ambient jet in low states and a shock in high states) or, if the same component is responsible for all variability patterns, its parameters change significantly, depending on the brightness of the source. Furthermore, the slopes obtained during the 2012 season substantially differ from those of the 2004 outburst (open symbols in Fig. 5). In Fig. 6 we plot relative SEDs of the variable component in CTA 102 during quiescence and the 2012 outburst from *Swift* UV to NIR bands, showing marked hardening of the SED during the high state, together with substantial curvature of the spectrum. It is tempting to suppose, as suggested in [18] for the case of BL Lac, that this spectral hardening is caused by a change of the viewing angle of the emitting zone, and the corresponding shift in frequency of the synchrotron spectrum due to Doppler boosting. Otherwise, these results imply that the populations of emitting electrons are very different in quiescence and outburst.

Simultaneous spectral hardening in the γ-ray region during the outburst is also apparent in Fig. 7. Notice that in this Figure we plot total observed flux densities, in contrast with Fig. 6.

3.2 Polarimetric Behavior

Figure 8 shows the distribution of normalized and absolute Stokes parameters of CTA 102 during both quiescence and different stages of the 2012 activity. We notice a marked drift of the center of gravity of the (q, u) points during and after the outburst compared to their pre-outburst positions. This may reflect the change of orientation of the jet itself. We also find four episodes of clockwise rotation (loops) in both the $q - u$ and $Q - U$ plots. All of these correspond to local increases of brightness (upper panel of the same figure). As in the case of S5 0716+71 [19], we use a model of a relativistic shock moving down a helical jet, or along helical magnetic field lines, to explain these rotations. It is a challenging task, since we are probably observing several separate events: spiral motion of a shock during the main flare of JD 2456188-6205, with three clockwise loops; a

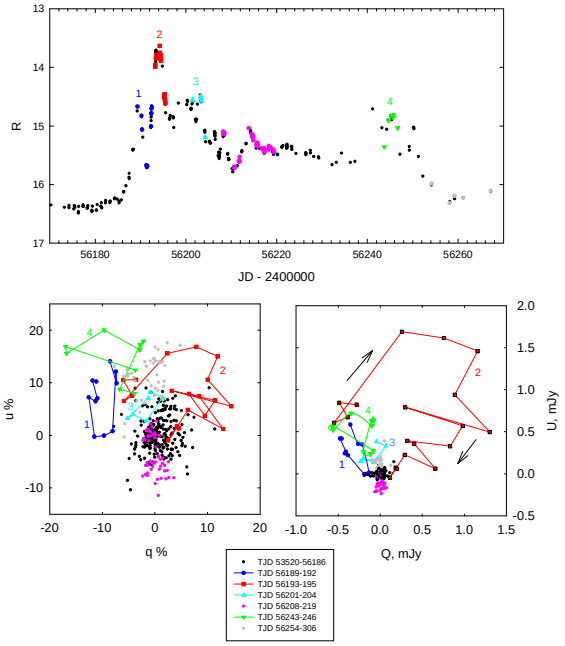

Figure 8. Lower left: normalized q and u Stokes parameters of the optical polarization of CTA 102. Lower right: the same for absolute Stokes parameters. Upper panel: R band light curve with the same color code as in lower panels. The top panel presents the R-band light curve, with intervals of time color-coded in the same way as the Stokes parameter plots.

flare without rotation, but with marked downward drift in the $q-u$ plane (JD 2456210-6220); a new prominent flare (JD 2456243–6248), again with a clockwise loop; and, following this on the descending branch of the light curve, upward movement in the $q-u$ plane. We notice that our finding of clockwise rotation of the polarization vector is supported by the detection of negative circular polarization in the 15 GHz radio emission of CTA 102 by Gabuzda et al. [20], who used the observation as evidence of a helical field. Thus it appears to be a persistent feature of this blazar.

3.3 Spectral Energy Distribution

The exceptional 2012 outburst of CTA 102 allows us to trace strong correlated changes of the spectral energy distribution of this blazar from γ-rays to near-infrared. As seen in Figures 6 and 7, the SED became harder when brighter in both the near-IR to UV and γ-ray spectral regimes. This is consistent with the same energy range of relativistic electrons emitting near-IR to UV synchrotron radiation and inverse Compton γ-rays.

During the height of the 2012 outburst, the peak frequency in the synchrotron SED was $\sim 1.5\times10^{14}$ Hz, while the γ-ray peak was $\sim 3\times10^{23}$ Hz. A likely source of seed photons for the inverse Compton scattering is IR blackbody radiation from hot dust in the inner few parsecs of the nucleus. (The high γ-ray to IR and γ-ray to X-ray flux ratios are difficult to reproduce with a synchrotron self-Compton model.) Malmrose et al. [21] have found a hot dust component of the SED with a temperature of $\sim$ 1200 K based on near- to far-IR observations. If we adopt Lorentz and Doppler factors of $\sim$ 20 [22], the peak of the dust-emitted spectrum is $\sim 5\times10^{14}$ Hz. If we take the square-root of the ratio of the deboosted γ-ray spectral peak, $\sim 1.5\times10^{22}$ Hz to the latter frequency, we estimate the Lorentz factor of the scattering electrons to be $\gamma \sim 5000$. The peak in the synchrotron SED is then reproduced if the magnetic field is $\sim$ 0.3 G, which is a reasonable value at a distance of $\sim$ 1–3 pc from the central engine.

Although the spectral hardening can be caused by an increase in the Doppler factor during the 2012 outburst, as mentioned above, this should increase the inverse Compton flux by a greater factor than it does the synchrotron flux. Figure 3 shows, however, that the optical and γ-ray amplitudes of the most prominent flare were roughly equal. It therefore seems more likely that the spectral hardening resulted from more efficient acceleration of the highest-energy particles during the outburst than during quiescent periods. Multi-waveband flux and polarization monitoring observations of future outburst(s) can determine whether this higher efficiency is related to the direction of the magnetic field in the jet.

Acknowledgements

This work was supported by RFBR foundation grants 12-02-00452 and 12-02-31193. The research at Boston University was funded in part by NASA Fermi Guest Investigator grants NNX08AV65G, NNX10AO59G, NNX10AU15G, NNX11AO37G, and NNX11AQ03G. The research at Steward Observatory was funded in part by NASA Fermi Guest Investigator grants NNX09AU10G and NNX12AO93G. The research at the IAA-CSIC is supported by the Spanish Ministry of Economy and Competitiveness and the Regional Government of Andalucía (Spain) through grants AYA2010-14844 and P09-FQM-4784, respectively. The Calar Alto Observatory is jointly operated by the Max-Planck-Institut für Astronomie and the Instituto de Astrofísica de Andalucía-CSIC.

References

[1] A. Sandage, J.D. Wyndham, ApJ **141**, 328 (1965)
[2] J.R.P. Angel, H.S. Stockman, ARA&A **18**, 321 (1980)
[3] R.L. Moore, H.S. Stockman, ApJ **243**, 60 (1981)
[4] A.J. Pica, A.G. Smith, J.R. Webb, R.J. Leacock, S. Clements, P.P. Gombola, AJ **96**, 1215 (1988)
[5] M. Villata, C.M. Raiteri, G. Sobrito, G. de Francesco, L. Lanteri, M. Cavallone, Astrophysical Letters and Communications **40**, 123 (2001)
[6] S. Katajainen, L.O. Takalo, A. Sillanpää, K. Nilsson, T. Pursimo, M. Hanski, P. Heinämäki, E. Kotoneva, M. Lainela, P. Nurmi et al., A&AS **143**, 357 (2000)
[7] A. Osterman Meyer, H.R. Miller, K. Marshall, W.T. Ryle, H. Aller, M. Aller, T. Balonek, AJ **138**, 1902 (2009)

[8] P.L. Nolan, D.L. Bertsch, C.E. Fichtel, R.C. Hartman, S.D. Hunter, G. Kanbach, D.A. Kniffen, Y.C. Lin, J.R. Mattox, H.A. Mayer-Hasselwander et al., ApJ **414**, 82 (1993)

[9] J.J. Blom, H. Bloemen, K. Bennett, W. Collmar, W. Hermsen, M. McConnell, V. Schoenfelder, J.G. Stacy, H. Steinle, A. Strong et al., A&A **295**, 330 (1995)

[10] P.L. Nolan, A.A. Abdo, M. Ackermann, M. Ajello, A. Allafort, E. Antolini, W.B. Atwood, M. Axelsson, L. Baldini, J. Ballet et al., ApJS **199**, 31 (2012)

[11] A.P. Marscher, S.G. Jorstad, V.M. Larionov, M.F. Aller, H.D. Aller, A. Lähteenmäki, I. Agudo, P.S. Smith, M. Gurwell, V.A. Hagen-Thorn et al., ApJ **710**, L126 (2010)

[12] I. Agudo, S.G. Jorstad, A.P. Marscher, V.M. Larionov, J.L. Gómez, A. Lähteenmäki, M. Gurwell, P.S. Smith, H. Wiesemeyer, C. Thum et al., ApJ **726**, L13 (2011)

[13] A.P. Marscher, S.G. Jorstad, ArXiv: 1005.5551 (2010), 1005.5551

[14] V. Larionov, D. Blinov, S. Jorstad, The Astronomer's Telegram **4397** (2012)

[15] R.A. Edelson, J.H. Krolik, ApJ **333**, 646 (1988)

[16] A.A. Breeveld, W. Landsman, S.T. Holland, P. Roming, N.P.M. Kuin, M.J. Page, *An Updated Ultraviolet Calibration for the Swift/UVOT*, in *American Institute of Physics Conference Series*, edited by J.E. McEnery, J.L. Racusin, N. Gehrels (2011), Vol. 1358 of *American Institute of Physics Conference Series*, pp. 373–376, 1102.4717

[17] V.M. Larionov, S.G. Jorstad, A.P. Marscher, C.M. Raiteri, M. Villata, I. Agudo, M.F. Aller, A.A. Arkharov, I.M. Asfandiyarov, U. Bach et al., A&A **492**, 389 (2008), 0810.4261

[18] V.M. Larionov, M. Villata, C.M. Raiteri, A&A **510**, A93 (2010), 0912.1867

[19] V.M. Larionov, S.G. Jorstad, A.P. Marscher, D.A. Morozova, D.A. Blinov, V.A. Hagen-Thorn, T.S. Konstantinova, E.N. Kopatskaya, L.V. Larionova, E.G. Larionova et al., ApJ **768**, 40 (2013), 1303.2218

[20] D.C. Gabuzda, V.M. Vitrishchak, M. Mahmud, S.P. O'Sullivan, MNRAS **384**, 1003 (2008), 0711.4572

[21] M.P. Malmrose, A.P. Marscher, S.G. Jorstad, R. Nikutta, M. Elitzur, ApJ **732**, 116 (2011), 1103.1682

[22] S.G. Jorstad, A.P. Marscher, M.L. Lister, A.M. Stirling, T.V. Cawthorne, W.K. Gear, J.L. Gómez, J.A. Stevens, P.S. Smith, J.R. Forster et al., AJ **130**, 1418 (2005), arXiv:astro-ph/0502501